

# Sensitivity of Unbiased Commercial P-channel Power VDMOSFETs to X-ray Radiation

G. S. Ristić, A. S. Jevtić, S. D. Ilić, S. Dimitrijević, S. Veljković, A. J. Palma, S. Stanković, and M. S. Andjelković

**Abstract** – The effect of X-rays on the p-channel power vertical double diffused metal-oxide-semiconductor field-effect transistors (VDMOSFETs) was investigated. The VDMOSFETs were irradiated without gate polarization using three different X-ray beams. Due to the polyenergetic nature of X-rays, their effect is much more complex than the effect of gamma radiation on transistors. The influence of X-rays on threshold voltage shift ( $\Delta V_T$ ) and on the creation of fixed traps (FTs) in gate oxide and on switching traps (STs) near and at oxide/semiconductor interface was analyzed. The effect of STs on  $\Delta V_T$  is more significant than in the case of  $\gamma$ -radiation. The obtained results showed that the sensitivity to radiation depends on the radiation energy, and they are in accordance with the theoretical predictions.

## I. INTRODUCTION

The metal-oxide-semiconductor field-effect transistors (MOSFETs) can operate in harsh environment where they are exposed to ionizing radiation, such as space, nuclear facilities, and radiotherapy units, and it is therefore important to know their behavior under higher levels of ionizing radiation [1-5].

In this paper, the influence of X-rays radiation on the commercial p-channel power Vertical Diffused MOSFETs (VDMOSFETs) is considered. The influence of X-rays radiation on power VDMOSFETs is not found in the literature. Because of the polyenergetic spectrum of X-ray radiation, it is much more complex and demanding than  $\gamma$ -radiation, so the challenge is greater. Otherwise, due to thick gate oxide commercial p-channel transistors can be considered as potential dosimeters of  $\gamma$ -radiation [6], but they have not been tested for X-rays.

The sensitivity of commercial P-channel VDMOSFETs

G. S. Ristić, A. S. Jevtić, S. D. Ilić, S. Dimitrijević, and S. Veljković are with the Department of Microelectronics, Faculty of Electronic Engineering, University of Niš, Niš, Serbia, E-mail: [goran.ristic@elfak.ni.ac.rs](mailto:goran.ristic@elfak.ni.ac.rs)

S. D. Ilić is also with Centre for Microelectronics, Institute for Chemistry, Technology and Metallurgy, University of Belgrade, Serbia, E-mail: [ilic.stefan@elfak.rs](mailto:ilic.stefan@elfak.rs)

A. J. Palma is with the University of Granada, Granada, Spain, E-mail: [ajpalma@ugr.es](mailto:ajpalma@ugr.es)

S. Stanković is with Department of Radiation and Environmental Protection, “Vinča” Institute of Nuclear Sciences, Belgrade, Serbia, E-mail: [srbas@vin.bg.ac.rs](mailto:srbas@vin.bg.ac.rs)

M. Andjelković is with the IHP - Leibniz-Institut für innovative Mikroelektronik, Frankfurt Oder, Germany, E-mail: [andjelkovic@ihp-microelectronics.com](mailto:andjelkovic@ihp-microelectronics.com)

to X-ray radiation, the behavior of the densities of positive radiation-induced fixed traps (FTs) in the gate oxide and switching traps (STs) at the interface, as well as the dependence of sensitivity on radiation energy were investigated. The transistors are irradiated without gate bias at three beam energies.

## II. EXPERIMENTAL DETAILS

Commercial p-channel VDMOSFETs, type IRF9520, were used. They are mounted in TO-220 plastic packaging, produced in standard silicon gate technology, and have an oxide thickness of about 100 nm. The transistors were irradiated without gate bias (all pins were shortconnected) at room-temperature with X-rays to the value of the air kerma of  $K_{air} = 50$  Gy in the Radiation and Environmental Protection Laboratory, Vinča Institute of Nuclear Science, Belgrade, Serbia. For irradiation, a Hopewell Design Beam Irradiator model x80-225 was used.

Air kerma,  $K_{air}$ , was measured directly with the dosimetric system containing the PTW UNIDOS Weblin electrometer and Exradin A3 ionization chamber. The transistors were irradiated at a distance of 35 cm, the  $K_{air}$  was measured at a distance of 50 cm, and then  $K_{air}$  recalculated for a distance of 35 cm using the quadratic law. If all the necessary constants were known, then it would be possible to calculate the absorbed dose in water,  $D_w$ , based on the  $K_{air}$  (Eq. 1 in Ref. [7]). However, since the dependence of  $D_w$  on  $K_{air}$ , based on the above mentioned equation (1), is linear, then  $K_{air}$  can be used instead of  $D_w$ .

Three RQR radiation qualities, which are used in general radiography, fluoroscopy and dental applications, were used. The mean energies are calculated by SpekCalc software that is free of charge for a research [8-10].

The characteristics of X-ray beams, the mean energies and air kerma rates are given in Table I.

TABLE I  
THE X-RAY BEAM TYPE, TUBE POTENTIAL ( $U_p$ ), TUBE CURRENT ( $I_p$ ), MEAN ENERGY ( $E_m$ ), AND AIR KERMA RATE ( $DK_{air}$ )

X-ray beam	$U_p$ (kV)	$I_p$ (mA)	$E_m$ (keV)	$DK_{air}$ (mGy/s)
RQR3	50	30	32.57	9.28
RQR8	100	30	50.82	26.45
RQR10	150	20	56.70	30.31

During radiation, an automatic system for measuring electrical characteristics were used. The custom made, switching and bias unit (SABU) [11], and for these experiments a specially designed and implemented printed circuit board with relays (PCBR), in which the VDMOSFETs were placed, are the parts of this system. The PCBR is connected with SABU via two DSUB cables, one DSUB-25 is for relay control and the other DSUB-9 is for transistors biasing. The SABU contains a PIC16F887 microcontroller that communicates with the computer via an FTDI chip. The source-measure unit (Keithley 2400 SMU) is connected with the computer using USB GPIB card. The entire system (SABU, PCBR and SMU) is controlled by C# program. The electrical diagram for the control of one relay on the SABU board can be seen in Fig. 1, and for the control of one VDMOSFET on PCBR during irradiation in Fig. 2.

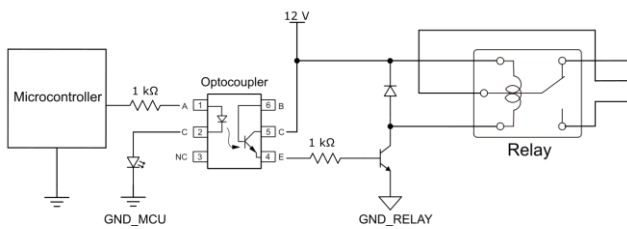


Fig. 1. The electrical diagram for the control of one relay in SABU.

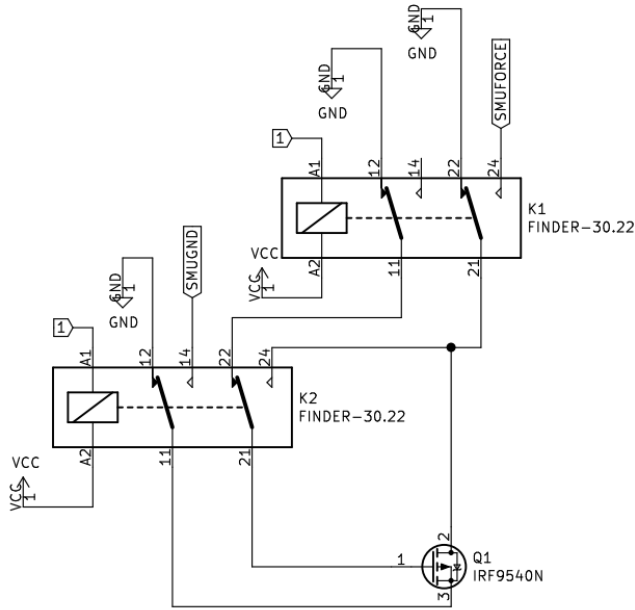


Fig. 2. The electrical diagram for the control of one transistor on PCBR during irradiation.

In order to faster measure the electrical characteristics of transistors, the gate and drain were shortconnected. The drain-source current,  $I_{DS}$ , was forced and the gate voltage,  $V_G$ , was measured. The threshold voltage,  $V_T$ , is determined

from the electrical transfer characteristics in saturation, as the intersection between  $V_G$  axis and the extrapolated linear region of the  $(I_{DS})^{1/2} - V_G$  curves using the least square method performed in the Octave 6.2.0 program [12]. The absolute values of  $V_T$  are used.

The midgap-subthreshold technique (MGT) [13] that determines the components of the threshold voltage shift,  $\Delta V_T$ , induced by positive fixed traps (FTs),  $\Delta V_{ft}$ , and switching traps (STs),  $\Delta V_{st}$ , was used. The MGT is based on the fact that positive FTs lead to a parallel shift of the subthreshold characteristics of the transistor, and STs lead to changes in the slope of its subthreshold characteristics. The relation between  $\Delta V_T$  and its components is:

$$\Delta V_T = \Delta V_{ft} + \Delta V_{st} . \quad (1)$$

The areal densities of FTs,  $\Delta N_{ft}$  [ $\text{cm}^{-2}$ ], and STs,  $\Delta N_{st}$  [ $\text{cm}^{-2}$ ] for p-channel MOSFETs can be found as

$$\Delta N_{ft} = \frac{C_{ox}}{e} \Delta V_{ft} , \quad \Delta N_{st} = \frac{C_{ox}}{e} \Delta V_{st} , \quad (2)$$

where  $C_{ox} = \epsilon_{ox}/t_{ox}$  is the gate oxide capacitance per unit area,  $\epsilon_{ox}=3.45 \cdot 10^{-13}$  F/cm is the silicon-dioxide permittivity, and  $e$  is the electron charge.

### III. RESULTS AND DISCUSSION

The results of threshold voltage shift during radiation are shown in Fig. 3. The RQR8 beam has the highest sensitivity. To find the sensitivity of transistors to radiation,  $S$ , we assumed that the dependence of  $\Delta V_T$  on  $K_{air}$  is linear:

$$\Delta V_T = S \cdot K_{air} . \quad (3)$$

The results showed very good agreement with the linear dependence and the  $r$ -square ( $r^2$ ) correlation coefficients were higher than 0.99 for all three cases. Sensitivity and  $r^2$  correlation coefficients are given in Table 2.

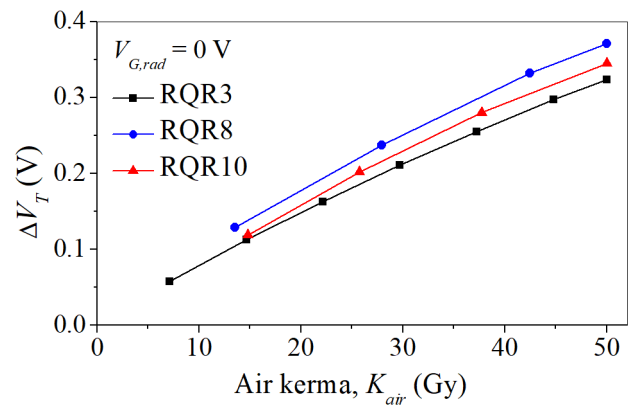


Fig. 3. Threshold voltage shift versus air kerma.

TABLE II  
SENSITIVITY AND R-SQUARE CORRELATION COEFFICIENTS.

X-ray beam	Sensitivity $S$ (mV/Gy)	$r^2$
RQR3	6.77	0.99723
RQR8	7.79	0.99466
RQR10	7.13	0.99709

The dependence of the density of fixed traps in the oxide (FTs), created under radiation influence, on air kerma is shown in Fig. 4. For the RQR8 beam, the  $\Delta N_{ft}$  has the highest values, while the values are almost the same for the other two beams.

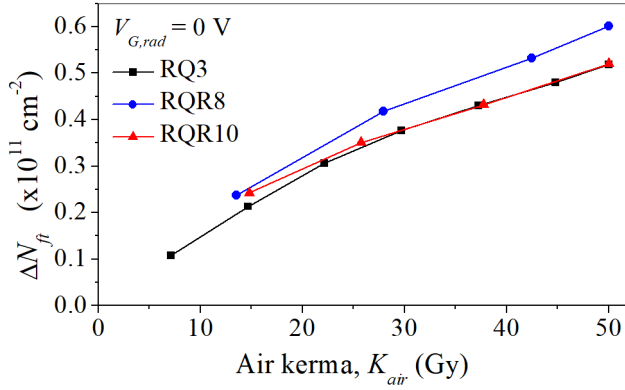


Fig. 4. Radiation-induced oxide fixed trap density versus air kerma.

Figure 5 shows the density of switching traps (STs) during X-ray radiation. It can be seen that the dependence on the beam energy is similar as in the case of  $\Delta V_T$  (Fig 3). If the density values are compared, the  $\Delta N_{ft}$  density is three times as high as the  $\Delta N_{st}$  density. However, these differences are not as significant as in the case of  $\gamma$ -radiation, where  $\Delta N_{st}$  is usually many times lower than  $\Delta N_{ft}$  [12]. It can be roughly said that FTs participate with three quarters, and STs with one quarter in the value of the  $\Delta V_T$ .

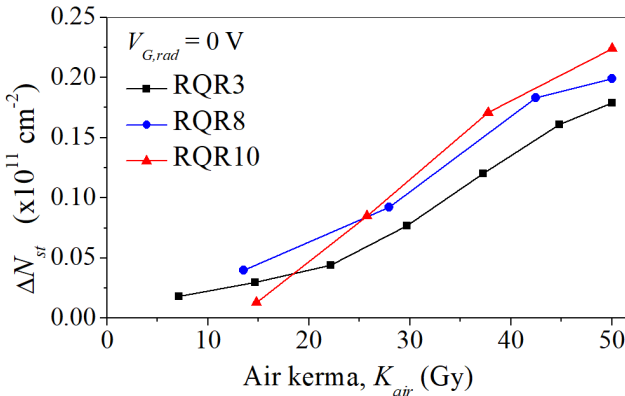


Fig. 5. Radiation-induced switching trap density versus air kerma.

The dependence of the sensitivity (Table II) on the mean beam energy (Table I) is shown in Fig. 6. It can be observed an energy dependence, as well as the maximum sensitivity for the RQR8 beam.

Sensitivity depends on  $\Delta N_{ft}$  and  $\Delta N_{st}$  densities, and these densities depend on the absorbed energy in the oxide. The more energy is absorbed in the oxide during radiation, the more FTs and STs are created, so the higher the  $\Delta V_T$ , and thus the higher the sensitivity. The energy absorbed per unit mass of irradiated matter at the point of interest represents absorbed dose.

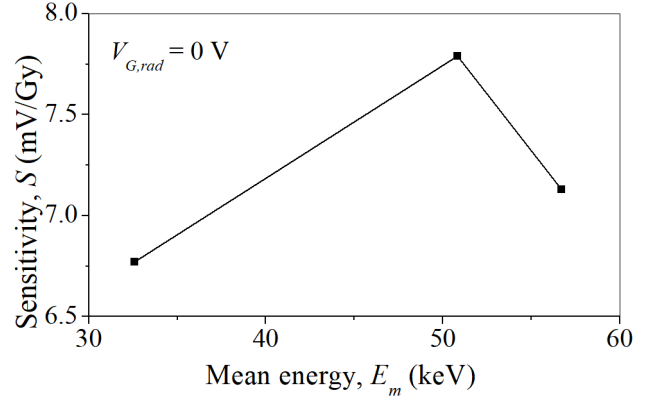


Fig. 6. Sensitivity versus mean beam energy.

To explain the dependence shown in the Fig. 6, we consider the following equation showing the dependence of absorbed dose in the matter,  $D$ , on absorbed dose in air,  $D_{air}$  [12]:

$$D = \frac{(\mu_{me}(E))_{matter}}{(\mu_{me}(E))_{air}} D_{air}, \quad (4)$$

where  $(\mu_{me}(E))_{matter}$  and  $(\mu_{me}(E))_{air}$  are the mass energy-absorption coefficients in a matter and in air, respectively.

Since  $D_{air} = K_{air}$  [12], then it can be written:

$$D = \frac{(\mu_{me}(E))_{matter}}{(\mu_{me}(E))_{air}} K_{air}. \quad (5)$$

It can be seen from Eq. (5) that the absorbed dose, at a given value of  $K_{air}$ , and thus the sensitivity, depends only on the ratio of these two coefficients. Fig. 7 shows the  $(\mu_{me}(E))_{silicon}$  and  $(\mu_{me}(E))_{air}$  coefficients for silicon (Si) and air, respectively (unfortunately we could not find for silicon-dioxide) [14]. As can be seen, the differences in these coefficients are significant below 100 keV, and after that the differences are negligible.

Fig. 8 displays the ratio of these coefficients  $((\mu_{me}(E))_{silicon}/(\mu_{me}(E))_{air})$  for various beam energies. As can be seen, the obtained energy distribution is similar to the energy distribution shown in Fig. 6. The difference is that

the peak in Fig. 8 is shifted to the left. The reason can be due to the difference in the mass energy-absorption coefficients of Si and SiO<sub>2</sub>. This ratio largely depends on the type of material for energies less than 100 keV.

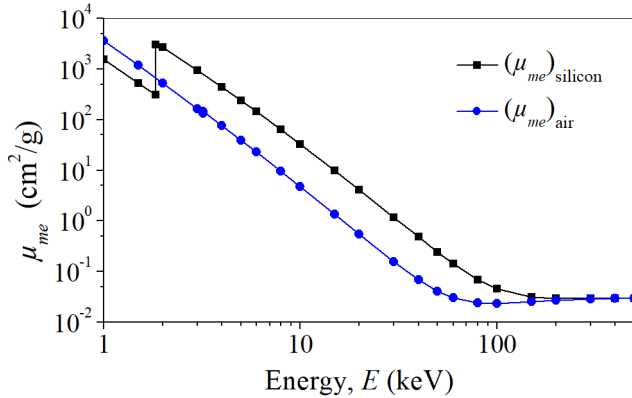


Fig. 7.  $(\mu_{me}(E))_{\text{silicon}}$  and  $(\mu_{me}(E))_{\text{air}}$  coefficients versus beam energy [14].

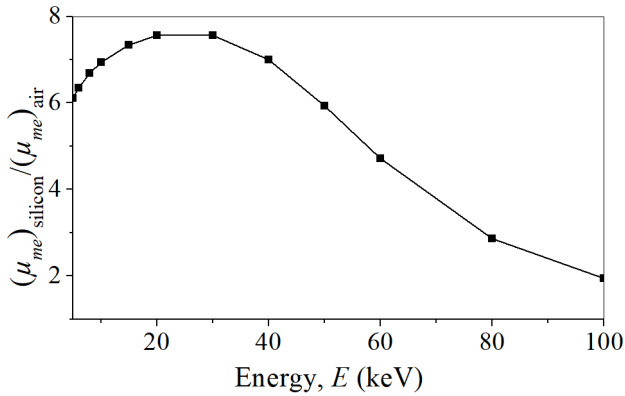


Fig. 8.  $(\mu_{me}(E))_{\text{silicon}}/(\mu_{me}(E))_{\text{air}}$  ratio versus beam energy.

#### IV. CONCLUSION

The specially printed circuit board with relays (PCBR) was designed and implemented for these experiments. It was used together with the previously specially designed SABU electrical circuit. The densities of radiation-induced fixed traps in the oxide and switching traps near and at SiO<sub>2</sub>/Si interface depend on the X-ray energy. The calculation of the absorbed dose in SiO<sub>2</sub>, as the medium responsible for the threshold voltage shift during radiation, is very complex in the case of X-rays, and there is no data in the literature. Therefore, the dependence of sensitivity on energy could not be precisely determined. The FTs participate with three quarters, and STs with one quarter in the threshold voltage shift, which is a significantly greater impact than in the case of  $\gamma$ -radiation.

#### ACKNOWLEDGEMENT

This work was supported in part by the European Union's Horizon 2020 research and innovation programme under grant agreement No. 857558, and the Ministry of Education, Science and Technology Development of the Republic of Serbia, under the project No. 43011.

#### REFERENCES

- [1] O. V. Aleksandrov, "Model of the behavior of MOS structures under ionizing irradiation", *Semiconductors*, 2014, vol. 48, pp. 505-510.
- [2] F. Jazaeri, C. Zhang, A. Pezzotta and C. Enz, "Charge-based modeling of radiation damage in symmetric double-gate MOSFETs", *IEEE Journal of the Electron Devices Society*, 2018, vol. 6, pp. 85-94.
- [3] A. P. Gnana Prakash, T. M. Pradeep, V. N. Hegde, N. Pushpa, P. K. Bajpai, S. P. Patel, T. Trivedi, and K. G. Bhushan, "Comparison of effect of 5 MeV proton and Co-60 gamma irradiation on silicon NPN rf power transistors and N-channel depletion MOSFETs", *Radiation Effects and Defects in Solids*, 2017, vol. 172, pp. 952-963.
- [4] C. Abbate, G. Busatto, D. Tedesco, A. Sanseverino, F. Velardi and J. Wyss, "Gate damages induced in SiC power MOSFETs during heavy-ion irradiation—Part II", *IEEE Transactions on Electron Devices*, 2019, vol. 66, pp. 4243-4250.
- [5] A. Dubey, R. Narang, M. Saxena, and M. Gupta, "Total ionizing dose effects in junctionless accumulation mode MOSFET", *Applied Physics A*, 2021, vol. 127, pp. 189-197.
- [6] M.M. Pejovic, "Application of p-channel power VDMOSFET as a high radiation doses sensor", *IEEE Transactions on Nuclear Science*, 2015, vol. 62, pp. 1905-1910.
- [7] C-M Ma, J. P. Seuntjens, "Mass-energy absorption coefficient and backscatter factor ratios for kilovoltage x-ray beams", *Physics in Medicine and Biology*, 1999, vol. 44, pp. 131-143.
- [8] G. G. Poludniowski, P. M. Evans, "Calculation of x-ray spectra emerging from an x-ray tube. Part I. electron penetration characteristics in x-ray targets", *Medical Physics*, 2007, vol. 34, pp. 2164-2174.
- [9] G. G. Poludniowski, "Calculation of x-ray spectra emerging from an x-ray tube. Part II. X-ray production and filtration in x-ray targets", *Medical Physics*, 2007, vol. 34, pp. 2175-2186.
- [10] G. Poludniowski, G. Landry, F. DeBlois, P. M. Evans and F. Verhaege, "SpekCalc: a program to calculate photon spectra from tungsten anode x-ray tubes", *Physics in Medicine and Biology*, 2009, vol. 54, pp. N433-N438.
- [11] S. Ilić, A. Jevtić, S. Stanković, G. Ristić, "Floating-gate MOS transistor with dynamic biasing as a radiation sensor", *Sensors*, 2020, vol. 20, pp. 3329-1-26.
- [12] G. S. Ristić, "Influence of ionizing radiation and hot carrier injection on metal-oxide-semiconductor transistors", *Journal of Physics D: Applied Physics*, 2008, vol. 41, pp. 023001-1-19.
- [13] P. J. McWhorter, P. S. Winokur, "Simple technique for separating the effects of interface traps and trapped-oxide charge in metal-oxide-semiconductor transistors", *Applied Physics Letters*, 1986, vol. 48, pp. 133 - 135.
- [14] J. H. Hubbell and S. M. Seltzer, "X-Ray Mass Attenuation Coefficients". Available at: <http://physics.nist.gov/xaamdi>